APPENDIX

Table of Contents

Appendix Figure Legends

Appendix Figure S1. (**A**) Venn diagrams showing intersections of miR-9-5p targets according to three different and independent target prediction tools (TargetScan, http://www.targetscan.org; miRanda, http://www.microrna.org and miRwalk, http://www.umm.uni-heidelberg.de/apps/zmf/mirwalk/). (**B**) Enriched KEGG pathways based on miR-9-5p *in silico* predicted targets by using the DAVID database 6.7 for analysis (Dennis et al, 2003). P values were determined with modified Fisher's exact test and corrected for multiple hypotheses testing with Benjamini-Hochberg FDR. Pathways with corrected $P < 0.05$ are depicted.

Appendix Figure S2. Position and evolutionary conservation of hsa-miR-9-5p seed sequence of 3´-UTRs of TGFBR2 and NOX4 mRNAs. TargetScan was used to search for miRNAs that could interact with the 3´-UTRs of human TGFBR2 and NOX4 mRNAs. Localization (depicted on top) and sequence alignments of miR-9-5p BSs in the 3´-UTR of TGFBR2 (**A**) and NOX4 (**B**). mRNAs from different species and the consensus sequences are shown. (**A**) The TGFBR2 3´-UTR (NM_003242) is 2,542 kilobase (kb) long and contains two predicted BSs for miR-9-5p (BS1 and BS2). The BS1 is poorly conserved and the BS2 is broadly conserved among vertebrates. (**B**) The NOX4 3´-UTR (NM_001143837) is 2,402 kb long and contains three predicted BSs for miR-9-5p (BS1, BS2 and BS3). All three BSs are broadly conserved among vertebrates. BSs for miR-9-5p in the 3´-UTRs of TGFBR2 and NOX4 from various species are boxed.

Appendix Figure S3. miR-9-5p expression levels in human lung fibroblasts after transfection. qRT-PCR analysis of miR-9-5p expression in HFL-1 cells transfected with 40 nM pre-miR-NC (control) or pre-miR-9-5p for 48 h. Bar graphs show mean ± SEM (n = 3); two-tailed Mann-Whitney U test; $^{*}P < 0.05$ compared to pre-miR-NC-transfected cells.

Appendix Figure S4. Effect of miR-9-5p over-expression on cell proliferation, cell viability and apoptosis. HFL-1 cells were transfected with 40 nM pre-miR-NC (control) or pre-miR-9-5p for 48 h. (**A**) *In vitro* growth curves represent the number of viable cells for each time. (**B**) Cell viability was determined using the XTT assay. The absorbance of the formazan product was measured at 450 nm, the reference wavelength used was 750 nm and the difference was represented for each time. (**C**) Cell death

was quantified by Annexin V-FITC and 7-AAD staining. PE Annexin V positive and 7-AAD negative cells (bottom right quadrant) are considered apoptotic. Data from one representative FACS experiment (numbers represent the percentage of cells in each quadrant) is depicted. Data are shown as media ± SEM (n = 3); two-tailed Mann-Whitney U test; no significant differences between control and pre-miR-9-5p-transfected cells were found.

Appendix Figure S5. Classification of human MCs by morphological characteristics and expression analysis. (**A**) Phase-contrast microscopy images of omentum-derived MCs and the two morphological patterns observed in confluent cultures of effluent-derived MCs. Scale bar = 50 μm. (**B**) qRT-PCR analysis of E-Cadherin (CDH1), Col1α1 and FN expression in omentum-derived MCs and in MCs isolated from effluents in dialysis fluid of patients undergoing PD. MCs isolated from effluents were classified in epithelioid (Epith) and non-epithelioid (Non-Epith) (fibroblast-like) according to the morphological characteristics and the transcription levels of epithelial (CDH1) and mesenchymal markers (Col1α1 and FN). Bar graphs show mean ± SEM (n = 3-5 samples per group); two-tailed Mann-Whitney U test; $^{*}P < 0.05$ compared to omentum-derived MCs.

A

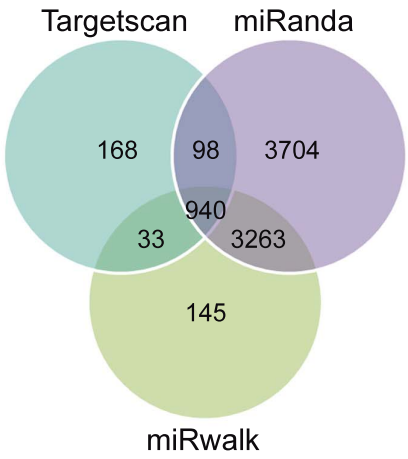

B

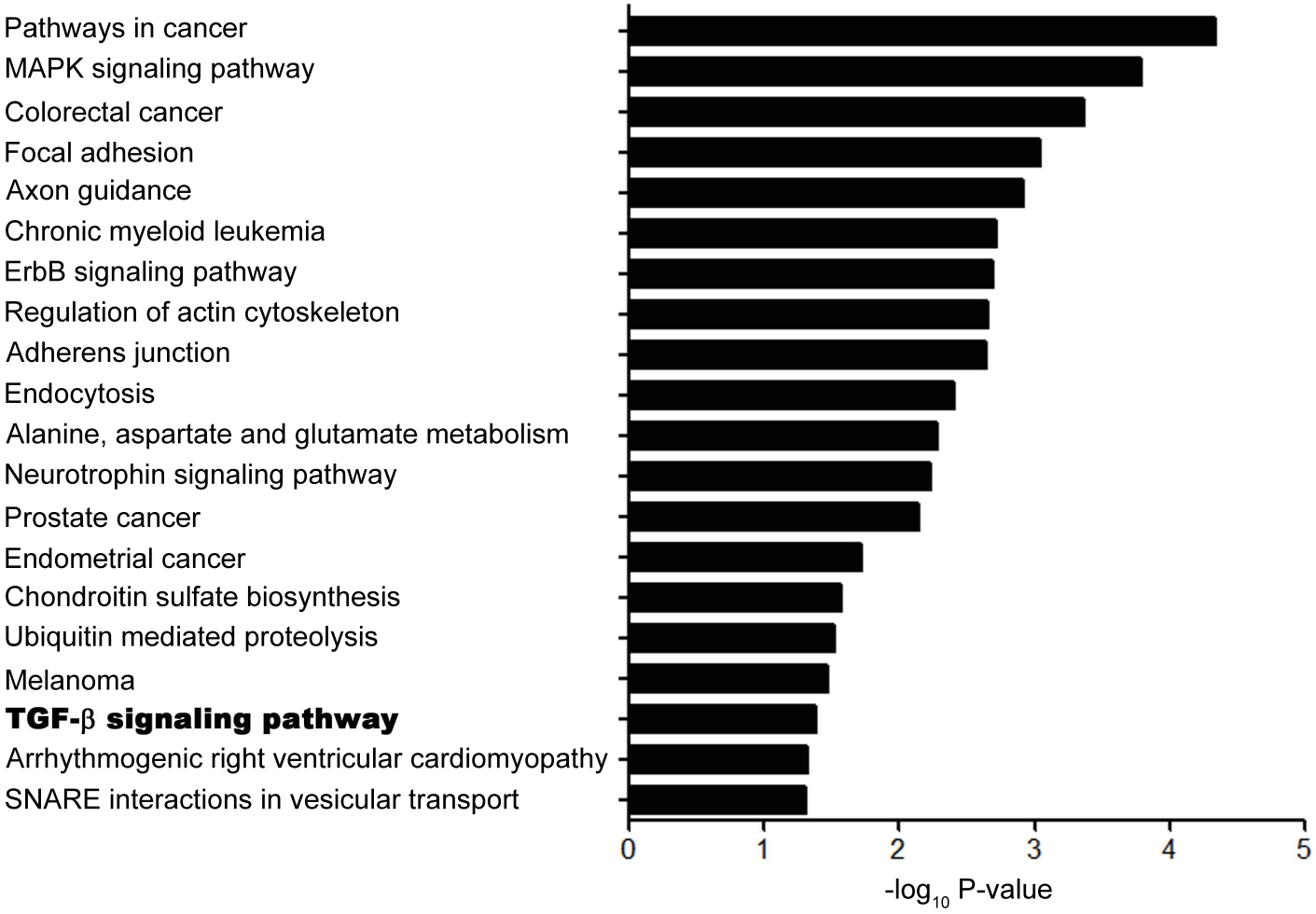

Appendix Fig S1

A

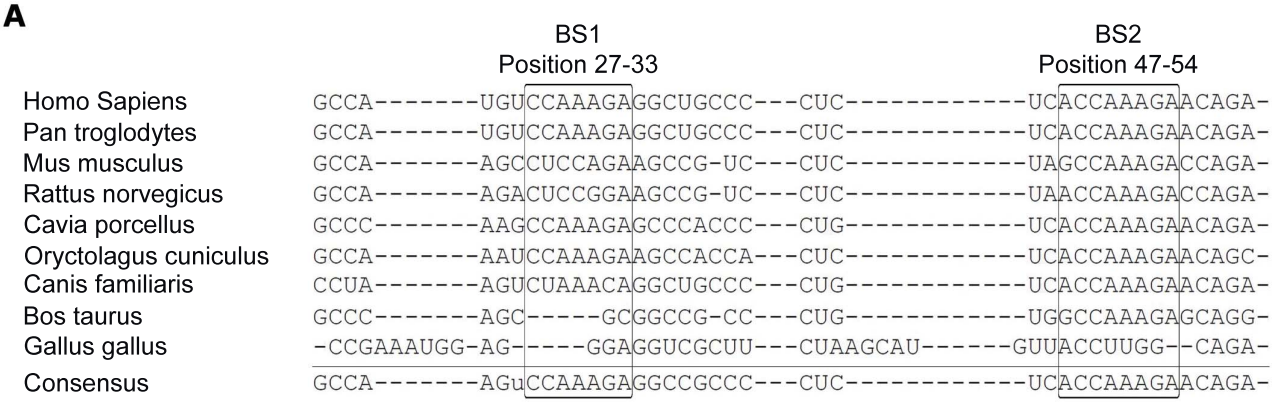

B

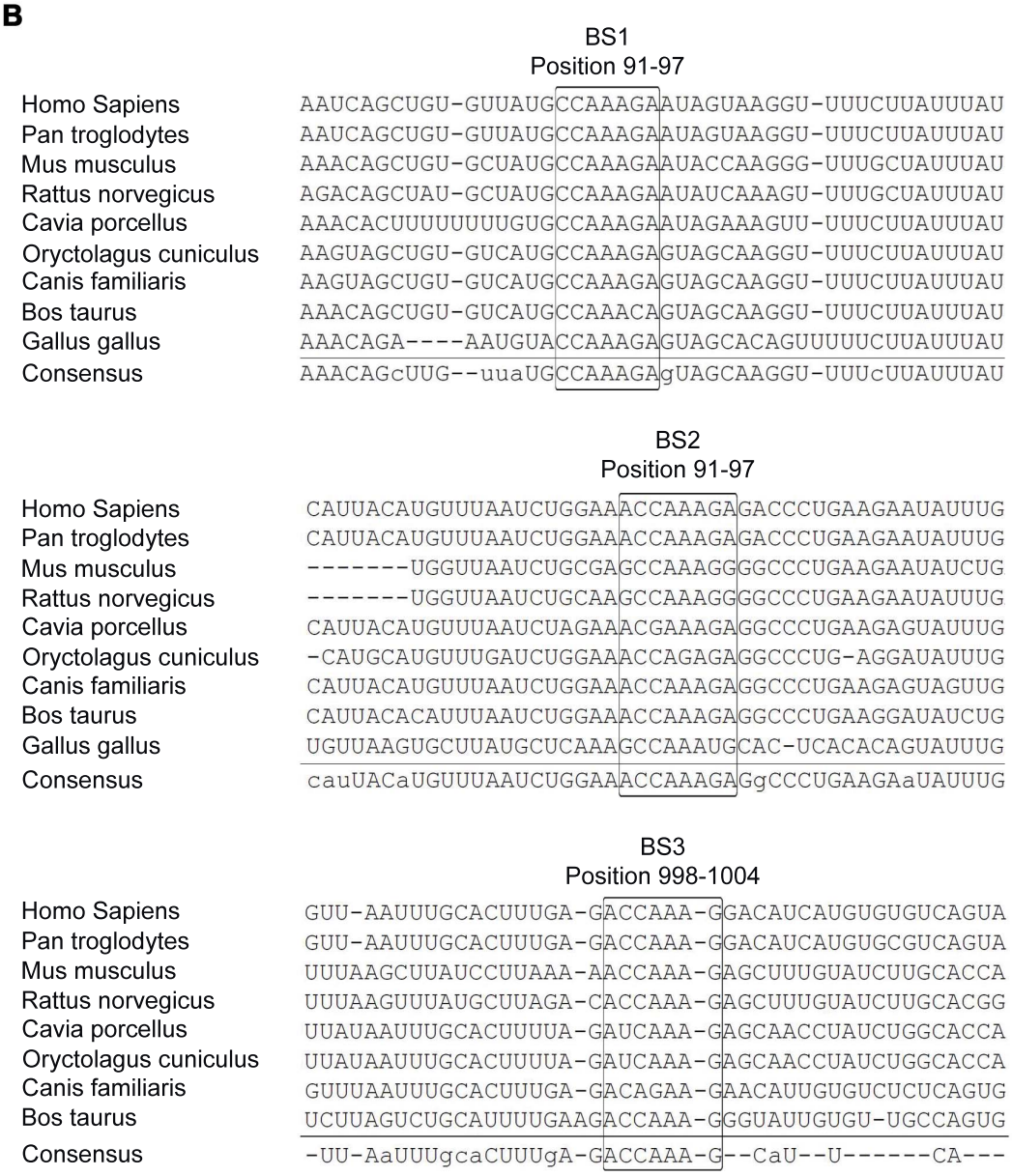

Appendix Fig S2

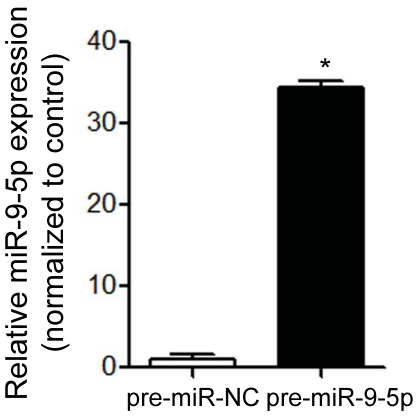

Appendix Fig S3

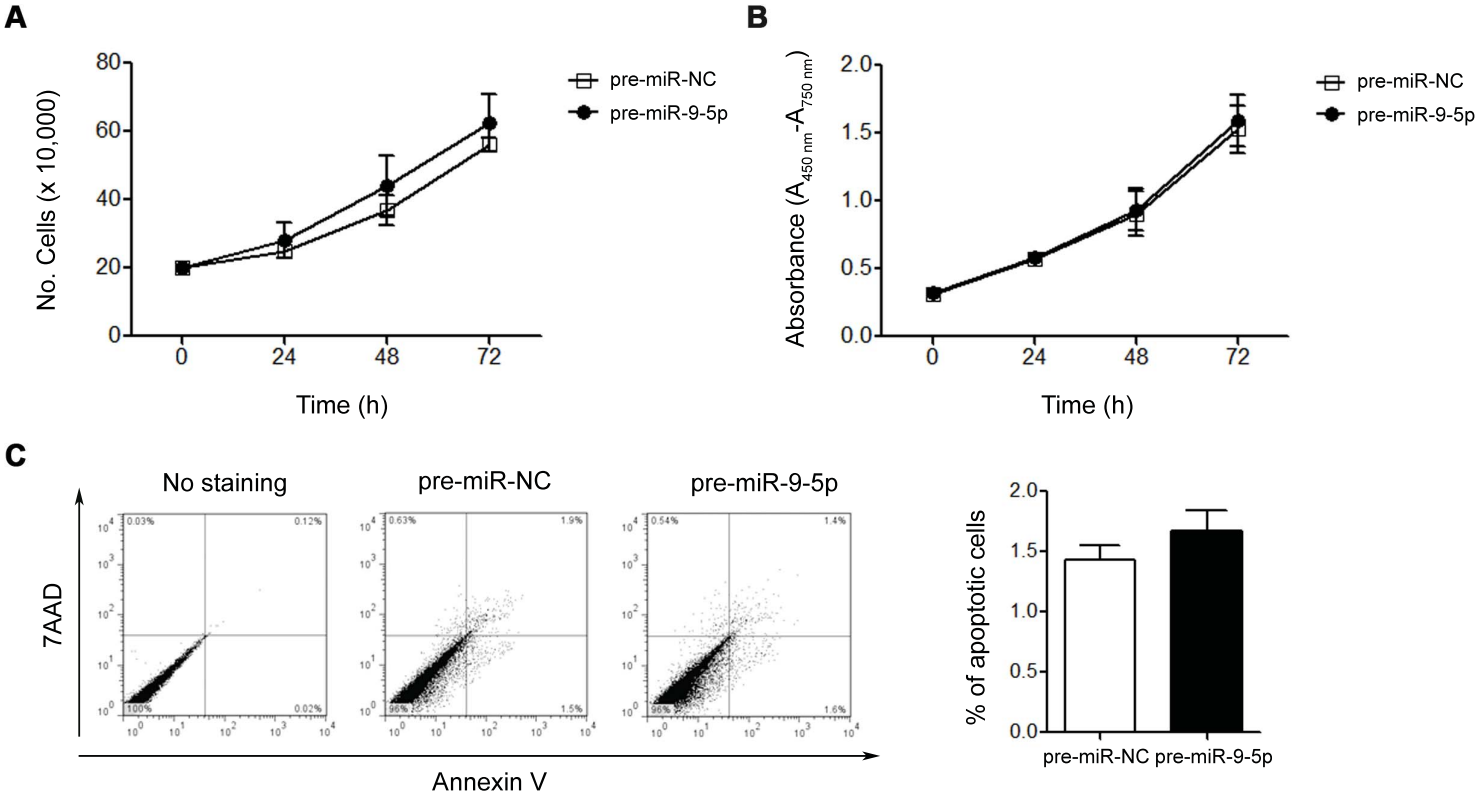

Appendix Fig S4

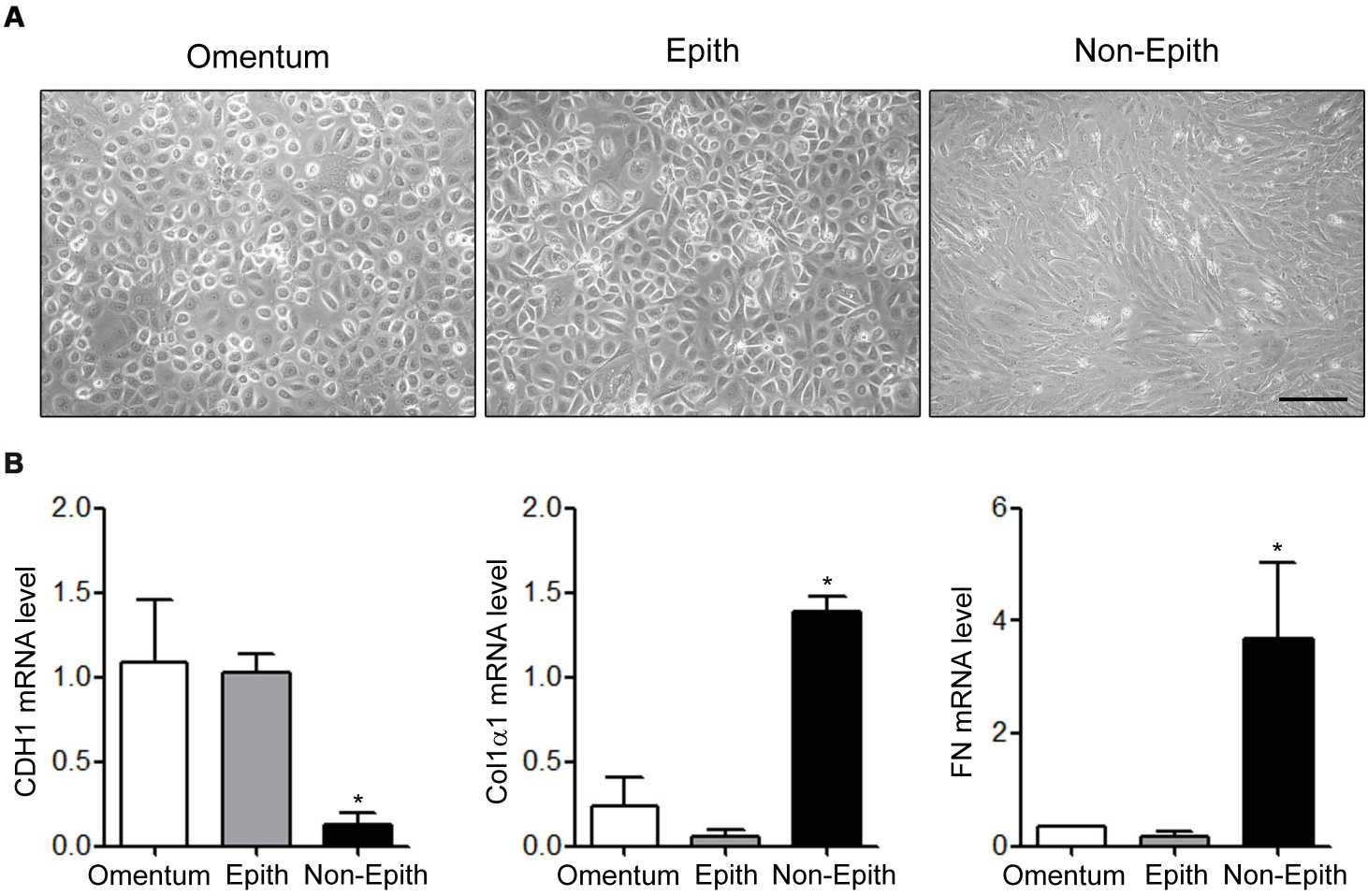

Appendix Fig S5